A New Four-Component L*-dependent Model for Radial Diffusion based on Solar Wind and Magnetospheric Drivers of ULF Waves

Kyle R. Murphy[1,2,3], Jasmine Sandhu[2], I. Jonathan Rae[2], Thomas Daggitt[4,5], Sarah Glauert[4], Richard B. Horne[4], Clare E. J. Watt[2], Sarah Bentley[2], Adam Kellerman[6], Louis Ozeke[7], Alexa J. Halford[8], Sheng Tian[9,10], Aaron Breneman[8], Leonid Olifer[7], Ian R. Mann[2,7], Vassilis Angelopoulos[6], John Wygant[10]

Affiliations:
1. Self - Independent Researcher, Thunder Bay, ON, Canada
2. Department of Maths, Physics and Electrical Engineering, Northumbria University, Newcastle Upon Tyne, United Kingdom
3. Department of Physics, Lakehead University, Thunder Bay, ON, Canada
4. British Antarctic Survey, Cambridge, UK
5. Department of Applied Mathematics and Theoretical Physics, University of Cambridge, Cambridge, UK
6. Department of Earth, Planetary, and Space Sciences, University of California, Los Angeles, CA, USA
7. Department of Physics, University of Alberta, Edmonton, Alberta, Canada
8. NASA Goddard Spaceflight Center, Greenbelt, MD, USA
9. Department of Atmospheric and Oceanic Sciences, University of California Los Angeles, CA, Los Angeles, USA
10. School of Physics and Astronomy, University of Minnesota, Minneapolis, MN, USA

Contents of this file

Introduction

This file contains 3 tables and 3 Figures.

Table S1 lists the satellites and instruments used in this study. Table S2 contains the fit and normalization coefficients for the linear regression D_{LL}^B and D_{LL}^Es models following the form of equations (1) and (2) in the manuscript (and below).

$$log_{10}(D_{LL}) = c + a_1 L^* + a_2 Sym\text{-}H + a_3 B_z + a_4 V + a_5 P_{dyn} \quad (1)$$

$$D_{LL} = 10^{c + a_1 L^* + a_2 SymH + a_3 B_z + a_4 V_t + a_5 P_{dyn}} \quad (2)$$

Figures S3 and S4 show the distribution of model residuals as a function of independent variable, L^*, $Sym\text{-}H$, B_z, V, and P_{dyn}, during geomagnetic storms and during geomagnetically quiet intervals. The residuals are calculated as the difference between the log10 of the modeled D_{LL}s and the satellite-derived D_{LL}s.

Figure S5 and Table S6 show the analysis used to remove the bias from the model residuals as a function of L^*. Figure S5 shows the Gaussian fits to the residuals and Table S6 contains the fit coefficients A0, A1, and A2 as a function of L^*. The coefficients allow researchers to remove the bias in the modeled D_{LL}^B and D_{LL}^Es in steps of 0.1 as a function of L^*. The Gaussian fit is of the form shown in equation (3).

$$f(r) = A_0 e^{(\frac{r - A_1}{A_2})^2} \quad (3)$$

Table S1. List of satellites and instruments used to derive magnetic and electric ULF PSD.

| Mission	Probe	Time Span	Instrument	Observation
GOES	15 (West)	2012-2020	magnetometer (MAG)	B
THEMIS	A, D, E	2013-2020	fluxgate magnetometer (FGM)	B
			electric field instrument (EFI)	E
Van Allen Probes	A, B	2012-2019	Electric and magnetic field instrument suite and integrated science (EMFISIS)	B
			Electric field and waves (EFW)	E

**Table S2.** Fit and normalization coefficients for the D_{LL} models.

	Independent Variable	Fitting Coefficient	Normalization Min	Normalization Max	Unit
D_{LL}^B	L*, a_1	4.2384115	3.00001	6.99997	-
	Sym-H, a_2	-6.0111539	-215.000	78.	nT
	Bz, a_3	-2.7546722	-30.4600	28.2700	nT
	V, a_4	1.3773411	239.800	924.400	km/s
	Pdyn, a_5	8.7776065	0.0500000	40.1100	nPa
	Constant, c	-0.33823768	-	-	-
D_{LL}^E	L*, a_1	4.6635730	3.00009	6.99997	-
	Sym-H, a_2	-3.2927855	-169.000	59.0000	nT
	Bz, a_3	-1.5571645	-19.9500	23.1500	nT
	V, a_4	1.7016774	244.100	924.400	km/s
	Pdyn, a_5	4.9563413	0.0700000	40.1100	nPa
	Constant, c	-1.9675309	-	-	-
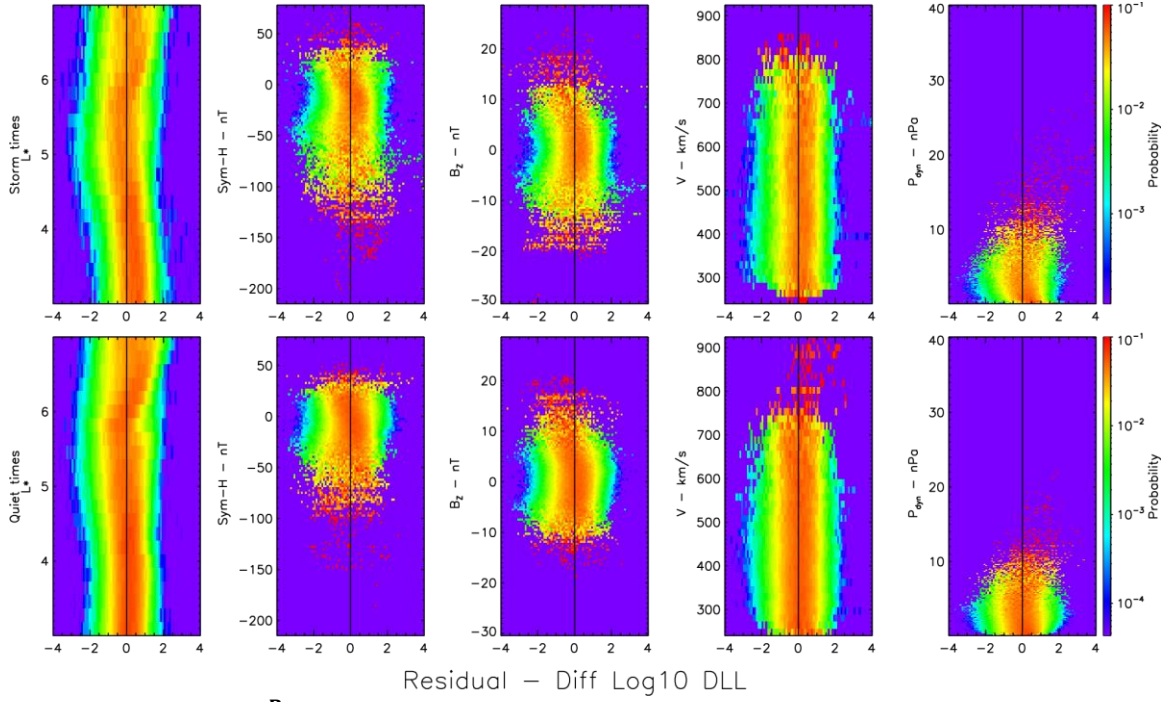
Figure S3. PDFs of D_{LL}^B model residuals calculated from the combined train and test data sets for each of the independent variables during geomagnetic storms and geomagnetically quiet times. The quiet times are defined as those times that are not part of geomagnetic storms.
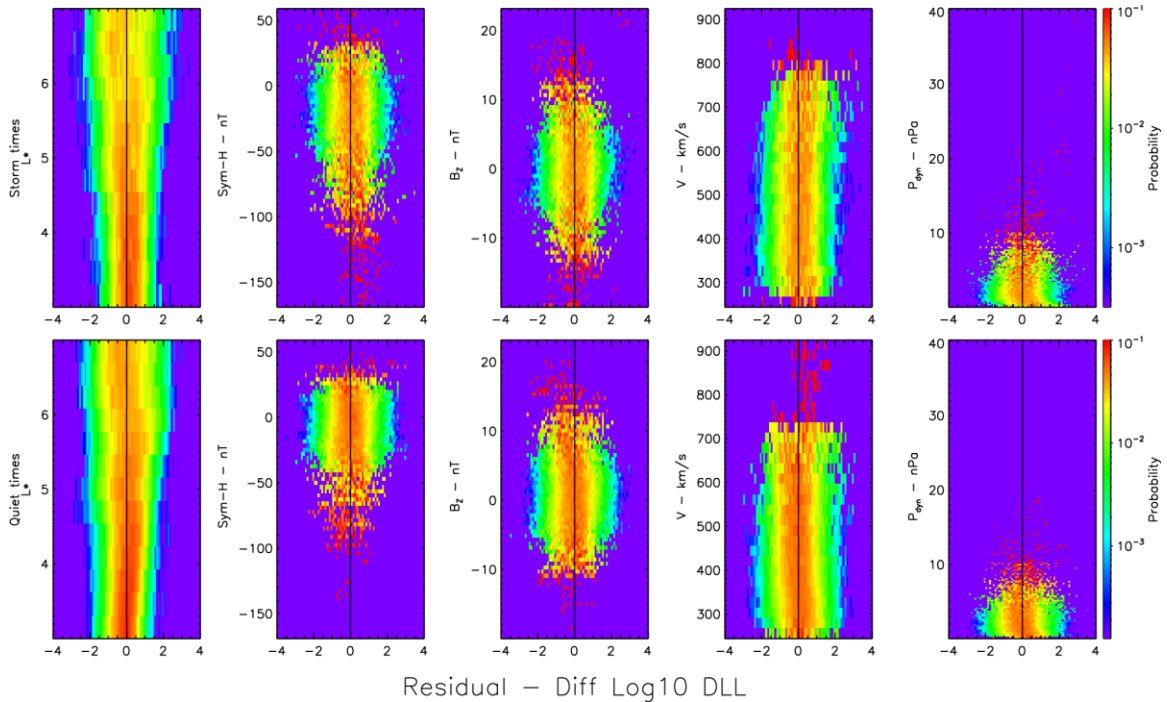
Figure S4. PDFs of D_{LL}^E model residuals calculated from the combined train and test data sets for each of the independent variables during geomagnetic storms and geomagnetically quiet times. The quiet times are defined as those times that are not part of geomagnetic storms.
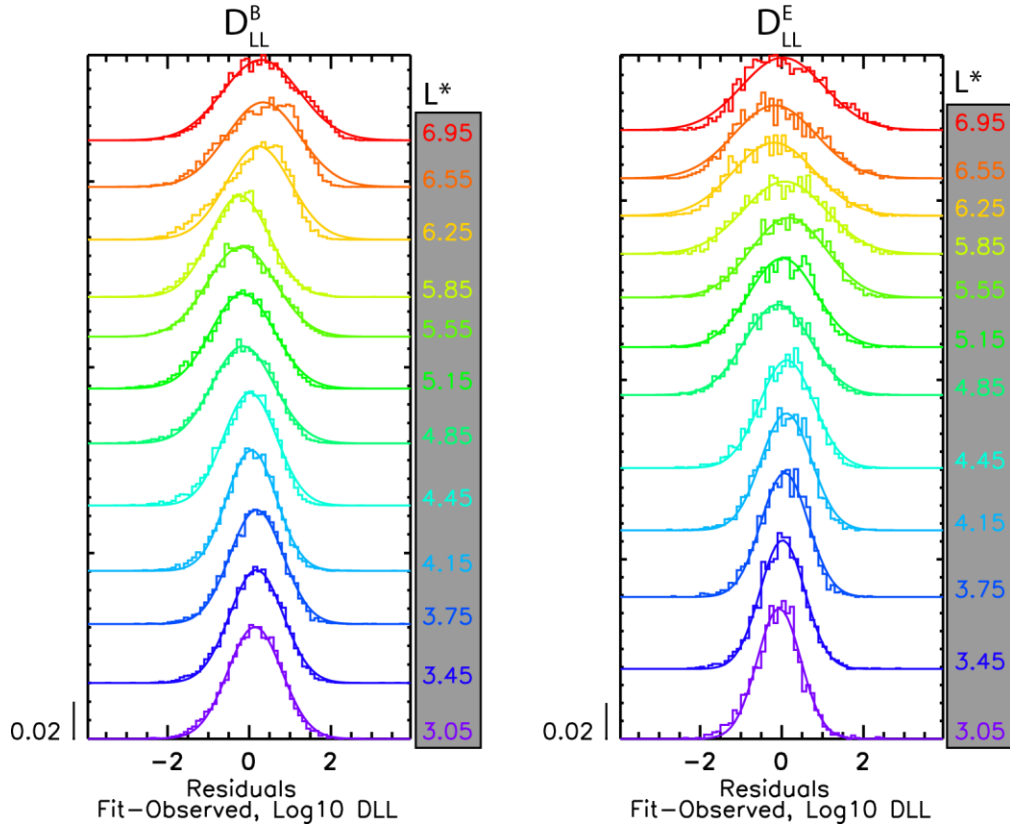
Figure S5. Example of fitting a Gaussian to the PDF of the residuals of the D_{LL}^B and D_{LL}^E models (left and right) as a function of L^*. Each color is a different L^*, as shown in the legends to the right of each panel. The PDFs are shown as histograms and the Gaussian fits as solid lines. The Gaussian fits provide a simple means to shift the residuals and remove the bias from the modelled D_{LL}s.

Table S6. Fit coefficients for the Gaussians as a function of L^*. The Gaussian fits are of the form shown in equation 3 of the manuscript and here. The fits are used to remove the bias in the modeled D_{LL}s. The Gaussian fits can also be used to generate an ensemble of D_{LL}s to run perturbed input ensemble simulations of radiation belt dynamics.

L*		DLLB			DLLE			L*		DLLB			DLLE		
Min	Max	A0	A1	A2	A0	A1	A2	Min	Max	A0	A1	A2	A0	A1	A2
3.0	3.1	0.060	0.141	0.660	0.073	-0.065	0.536	5.0	5.1	0.051	-0.165	0.778	0.051	-0.048	0.788
3.1	3.2	0.062	0.174	0.640	0.071	-0.038	0.555	5.1	5.2	0.051	-0.157	0.778	0.050	0.022	0.818
3.2	3.3	0.062	0.179	0.640	0.072	-0.019	0.545	5.2	5.3	0.050	-0.165	0.805	0.050	0.059	0.809
3.3	3.4	0.062	0.174	0.644	0.072	-0.019	0.551	5.3	5.4	0.048	-0.161	0.842	0.048	0.128	0.837
3.4	3.5	0.061	0.179	0.654	0.072	0.019	0.548	5.4	5.5	0.048	-0.149	0.842	0.046	0.196	0.878
3.5	3.6	0.061	0.186	0.650	0.070	0.020	0.569	5.5	5.6	0.048	-0.19	0.829	0.044	0.170	0.916
3.6	3.7	0.061	0.189	0.652	0.070	0.053	0.562	5.6	5.7	0.050	-0.272	0.795	0.042	0.159	0.966
3.7	3.8	0.061	0.181	0.651	0.069	0.073	0.576	5.7	5.8	0.053	-0.291	0.751	0.041	0.100	0.988
3.8	3.9	0.062	0.18	0.647	0.068	0.042	0.589	5.8	5.9	0.054	-0.228	0.724	0.040	0.072	1.011
3.9	4.0	0.061	0.163	0.649	0.065	0.073	0.612	5.9	6.0	0.055	-0.057	0.714	0.041	-0.042	0.998
4.0	4.1	0.062	0.108	0.648	0.065	0.097	0.613	6.0	6.1	0.053	0.063	0.741	0.040	-0.122	1.009
4.1	4.2	0.065	0.058	0.610	0.065	0.111	0.613	6.1	6.2	0.052	0.148	0.770	0.041	-0.162	0.969
4.2	4.3	0.065	0.049	0.601	0.062	0.128	0.642	6.2	6.3	0.050	0.229	0.791	0.041	-0.186	0.997
4.3	4.4	0.063	0.056	0.620	0.060	0.125	0.675	6.3	6.4	0.048	0.257	0.842	0.042	-0.175	0.953
4.4	4.5	0.061	0.022	0.653	0.060	0.125	0.662	6.4	6.5	0.046	0.325	0.875	0.040	-0.177	1.005
4.5	4.6	0.058	0.009	0.688	0.057	0.097	0.697	6.5	6.6	0.046	0.341	0.891	0.041	-0.166	1.00
4.6	4.7	0.054	-0.047	0.736	0.053	0.000	0.761	6.6	6.7	0.044	0.339	0.930	0.040	-0.138	1.012
4.7	4.8	0.054	-0.092	0.742	0.052	-0.071	0.775	6.7	6.8	0.043	0.332	0.956	0.041	-0.105	0.993
4.8	4.9	0.052	-0.149	0.763	0.050	-0.095	0.803	6.8	6.9	0.043	0.32	0.949	0.041	-0.056	0.983
4.9	5.0	0.052	-0.145	0.769	0.051	-0.050	0.793	6.9	7.0	0.043	0.292	0.938	0.040	0.026	1.005